Article ID: 1006-8775(2012) 02-0146-16

NUMERICAL SIMULATION ON RE-INTENSIFICATION OF TROPICAL REMNANT RE-ENTERING THE SEA: A CASE STUDY

ZENG Zhi-hua (曾智华)[1, 2], CHEN Lian-shou (陈联寿)[3]

(1. Nanjing University of Information Science and Technology, Nanjing 210044 China; 2. Shanghai Typhoon Institute, Laboratory of Typhoon Forecast Technique/China Meteorological Administration, Shanghai 200030 China; 3. Chinese Academy of Meteorological Sciences, China Meteorological Administration, Beijing 100081 China)

Abstract: When Typhoon Toraji (2001) reached the Bohai Gulf during 1-2 August 2001, a heavy rainfall event occurred over Shandong province in China along the gulf. The Advanced Research version of the Weather Research and Forecast (WRF-ARW) model was used to explore possible effects of environmental factors, including effects of moisture transportation, upper-level trough interaction with potential vorticity anomalies, tropical cyclone (TC) remnant circulation, and TC boundary-layer process on the re-intensification of Typhoon Toraji, which re-entered the Bohai Gulf after having made a landfall. The National Centers for Environmental Prediction (NCEP) global final (FNL) analysis provided both the initial and lateral boundary conditions for the WRF-ARW model. The model was initialized at 1200 UTC on 31 July and integrated until 1200 UTC on 3 August 2001, during which Toraji remnant experienced the extratropical transition and re-intensification. Five numerical experiments were performed in this study, including one control and four sensitivity experiments. In the control experiment, the simulated typhoon had a track and intensity change similar to those observed. The results from three sensitivity experiments showed that the moisture transfer by a southwesterly lower-level jet, a low vortex to the northeast of China, and the presence of Typhoon Toraji all played important roles in simulated heavy rainfall over Shandong and remnant re-intensification over the sea, which are consistent with the observation. One of the tests illustrated that the local boundary layer forcing played a secondary role in the TC intensity change over the sea.

Key words: tropical cyclone remnant; structure and intensity change; landfall; numerical simulation; returning to the sea

CLC number: P444 **Document code:** A **doi:** 10.3969/j.issn.1006-8775.2012.02.005

1 INTRODUCTION

Tropical cyclones (TCs) are warm-core systems that are among the most devastating of natural disasters, frequently causing loss of human life and serious economic damage. TCs are driven by the release of large amount of latent heat of condensation, which occurs when moist air is carried upwards and results in water-vapor condensation. The process of water-vapor budget can affect TC intensity by forming a warm core (Chen[1]). After making landfall, TCs often weaken and decay due to land surface friction and reduced moisture transfer from the ocean (Powell et al.[2-4], Tuleya et al.[5], Tuleya[6]). However, a landfalling TC can have large amount of rainfall, which may result in accumulated surface water on the ground. Shen et al.[7] studied the impact of surface water over land on the weakening of landfalling hurricanes with the hurricane model of the Geophysical Fluid Dynamics Laboratory (GFDL). They found a local surface cooling area near the hurricane core, with the coldest part behind and on the right hand side of the hurricane center. They showed that the water can significantly slow down landfall decay due to large entropy flux from the water surface. A landfalling TC remnant may receive a large amount of vapor supply in some other ways, say from large lakes, reservoirs, and oceanic moisture air with lower jets of southeasterly and southwesterly winds, which

Received 2011-09-30; **Revised** 2012-02-17; **Accepted** 2012-04-15

Foundation item: National Basic Research Program of China (973 Program) (2009CB421500); Natural Science Foundation of China (40875039, 40730948, 40921160381); Projects for Public Welfare (Meteorology) of China (GYHY201006008)

Biography: ZENG Zhi-hua, Ph.D., primarily undertaking research on tropical cyclone theory and numerical simulation.

Corresponding author: ZENG Zhi-hua, e-mail: zengzh@mail.typhoon.gov.cn

might sustain the TC for a long period of time over land (Chen[8]). Ding et al.[9] investigated the influence of moisture transportation on a tropical depression in Henan province of China. They found that the water vapor was transferred by the easterly wind at lower levels. Tan et al.[10] showed that the southerly low-level jet (LLJ) close to the edge of the subtropical high pressure was the major water-vapor transport belt, determined through water-vapor diagnose of the extratropical transition (ET) processes of landfalling Typhoon Freda (1967). Environmental humidity has a positive correlation to lagged TC intensity change (Emanuel[11], Holland[12]). Wang et al.[13] also considered that a large amount of moisture transfer of Typhoon Songda (2004) played an important role in producing remote heavy rainfall over Japan.

Holland and Merrill[14] showed that the interaction between a TC and a passing trough could enhance the outflow jet of the TC, enlarging core-region convection and initiating the deepening of the cyclone. Molinari and Vollaro[15-16] found that the upper-level eddy flux convergence of momentum occurred during the intensifying period of Hurricane Elena (1985), indicating that the upper-tropospheric trough with a positive potential vorticity (PV) anomaly played an important role in the re-intensification of Elena. Persing et al.[17] also showed that the upper-tropospheric trough played a minimal role in intensification of Hurricane Opal (1995). Hanley et al.[18] examined 121 Atlantic TCs in an attempt to differentiate between troughs that lead to intensification (good troughs) and those that lead to decay (bad troughs). However, the ‘‘bad trough’’ or ‘‘good trough’’ for TC intensity is still under debate, and is likely to be case-dependent and phase-locked.

Guo et al.[19] explored, based on statistical studies, the intensity change of TCs that landed in China and then entered the sea. Their results indicated that 24% of the storms that reinforced remarkably when entering the sea again took place in waters off the north of China, and their ration of re-intensification is much higher than those that made landfall in Hainan or Taiwan Islands. Typhoon Toraji landed during July-August 2001 and the remnant moved north with the re-intensification while entering the Bohai Gulf again. In order to investigate the impacts of moisture transfers on Typhoon Toraji intensity change from environmental southwesterly flows and flows the storm produced, a northeast vortex, and latent-heat release induced by the oceanic process, a series of sensitivity simulations were undertaken for the initial atmospheric states in which the dynamics and/or the moisture of each of the systems were modified. Significant differences between the control simulation and a sensitivity test were observed, which indicates that the modification has a remarkable impact on the evolution of the remnant of Typhoon Toraji.

In section 2, descriptions are given for the selected case of Typhoon Toraji in July-August 2001, the data used, and model configuration. Section 3 presents a brief analysis of a set of sensitivity tests designed to verify the roles of water-vapor transfers from environmental and/or the tropical cyclone remnant, together with a low drag coefficient scheme on TC intensity change. Section 4 describes the effect of each sensitivity test on precipitation distribution. Section 5 introduces the column-integrated moisture flux divergence to measure whether the transported moisture contributes to precipitation and TC intensity change in each of the tests. Section 6 presents conclusions and discussions of our findings.

2 CASE STUDY, MODEL SETUP, AND RESULTS OF CONTROL RUN

The tropical remnant of Typhoon Toraji (2001) provide an excellent case for studying TC extratropical transitions (ET) and processes associated with the TC entering the sea after making a landfall. A traditional synoptic diagnosis of this case is carried out, with the focus on the observed and investigated structures of the storm. The dataset and model setup are described briefly in sections 2b and 2c. The results of the control simulation are given in section 2d.

2.1 *Case description*

Although this study focuses on the re-intensification phase of tropical remnant from Typhoon Toraji after it entered the sea, a description of the TC history is necessary for understanding the importance of the remnant tropical vortices to the processes under investigation. Understanding of the evolution of the TC circulation, a low vortex to the northeast of China, and the moisture structure associated with the storm are of great importance in conceptualizing the sensitivity tests presented in section 3.

Typhoon Toraji began its life cycle as a tropical wave over the east coast of the Philippine Islands on 23 July 2001. The easterly wave began to organize nearby convection on 25 July, which was classified as tropical storm after that day (Figure 1). Moving toward northwest across the equatorial Pacific, the storm gradually developed into a typhoon. At this time, Typhoon Toraji achieved the maximum wind of approximately 40 m s^{-1}, and the central minimum pressure estimated to be around 965 hPa. The storm made landfall at Hualian in Taiwan in the morning of 30 July, with a central maximum wind of about 35 m s^{-1} and a minimum pressure at about 970 hPa. After crossing the Taiwan Strait, the TC landed in Lianjiang, Fujian at 1800 UTC on 30 July with a central maximum wind of about 30 m s^{-1} and a minimum pressure at about 985 hPa.

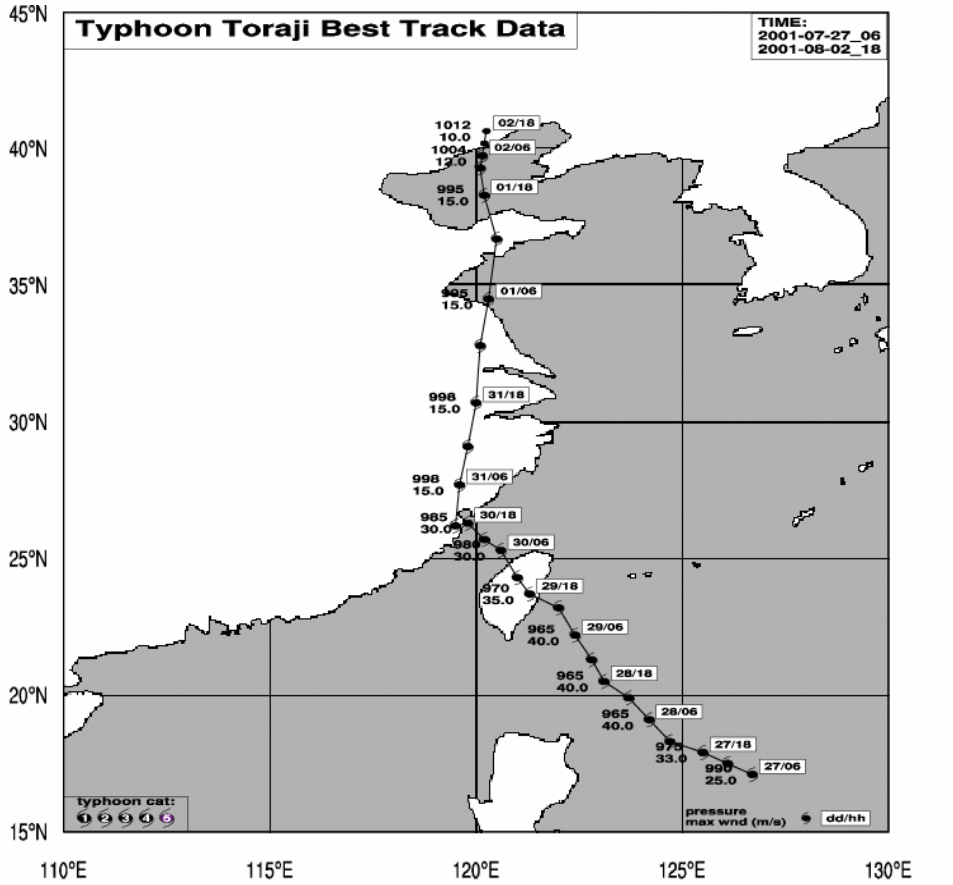

Figure 1. The best track for Typhoon Toraji. Plotting starts at 0600 UTC on 27 July in the east coast of the Philippine Islands and ends at 1800 UTC on 2 August in the northeast of China. Closed circles indicate 0600 and 1800 UTC positions of the TC, open squares indicate time, and digital values indicate minimum pressure and maximum wind of the TC, respectively.

Storm Toraji continued to track northward crossing Zhejiang, Jiangsu, and Shandong provinces until 0600 UTC on 1 August, with the lowest central pressure of 995 hPa. However, upon reaching the Bohai Gulf, the tropical remnant of Toraji experienced the ET process and re-intensification evolution, reaching the lowest central pressure of 993 hPa off the coast of the Bohai Gulf at 1200 UTC on 1 August, under the influence of a strong upper-level trough and/or a northeast vortex over Northeast China. In the following 30 hours, the system weakened to a minimum central pressure of 1012 hPa. During the life cycle of the tropical remnant moving northward, the storm resulted in heavy rainfall over East and Northeast of China and caused accumulated precipitation of about 100–200 mm over the central Jiangsu province and in Yantai of Shandong province.

2.2 *Data sources*

We use the National Centers for Environmental Prediction (NCEP) global final (FNL) analysis dataset at 1°×1° grid and 6-h interval for both the initial and lateral boundary conditions of the model. This dataset is archived by the National Center for Atmospheric Research (NCAR). The model is the Advanced Research WRF (ARW) developed at the NCAR (Skamarock et al.[20]); more detail will be given in section 2.3. Other datasets include the best track information from the *Typhoon Year Book* and the *Tropical Cyclone Year Book* published by the China Meteorological Press.

For consistency, sea-surface temperature (SST) used in the model simulation is taken from the NCEP real-time objective SST analysis with 0.5°×0.5° horizontal grid spacing. The SST remains the same throughout the integration. Although some studies showed that the influence of variable SST on the TC system is non-negligible, our on-going research shows that the perturbation to SST is quite small.

2.3 *Model description*

All simulations for this study were performed using version 3.0 of the WRF-ARW. The model is a three-dimensional, fully compressible, non-hydrostatic model formulated using a terrain-following mass coordinate in the vertical. The model physics include the Ferrier cloud microphysics scheme (Ferrier[21]), the Rapid Radiative Transfer Model (RRTM) for longwave radiation (Mlawer et al.[22]), the Goddard shortwave radiation scheme

(Chou and Suarez[23]), the Monin–Obukhov surface flux calculation over the ocean, the Rapid Update Cycle (RUC) land surface model (Smirnova et al.[24, 25]), the Yonsei University (YSU) planetary boundary layer scheme (Hong et al.[26]), and the Kain–Fritsch cumulus parameterization scheme (Kain and Fritsch[27]) for subgrid-scale deep convection. Only a high-resolution domain of terrain height and dominant category was used in this study. The domain has 500 × 450 grid points, and is centered at 30°N, 120°E with a horizontal grid of 9 km. The model was run with 34 unevenly distributed vertical levels, with a higher resolution in the planetary boundary layer and the model top at 50 hPa.

2.4 *Control simulation*

All of the simulations for this study are initialized at 1200 UTC on 31 July and integrated for 72 h with a 30-second time step. At the initial time, Toraji is at a relatively weak stage of its life cycle. As shown in Figures 2a and 2b for best track maps and intensity plots, respectively, Toraji was located at 29.1°N and 119.8°E in Fujian (Figure 2a), with a minimum mean sea-level pressure (MSLP) of 998 hPa (Figure 2b) and mean near-core wind of 12 m s^{-1} (not shown). Figure 2 indicates that the control simulation's track and intensity change almost coincide with the best track data. Note that the trend and phase of the cyclone's intensity change are close to the observed, although the bogus initialization was not used in the simulation. The time of re-intensification of tropical remnant is at 24-h simulation, which is also similar to the observed best track data.

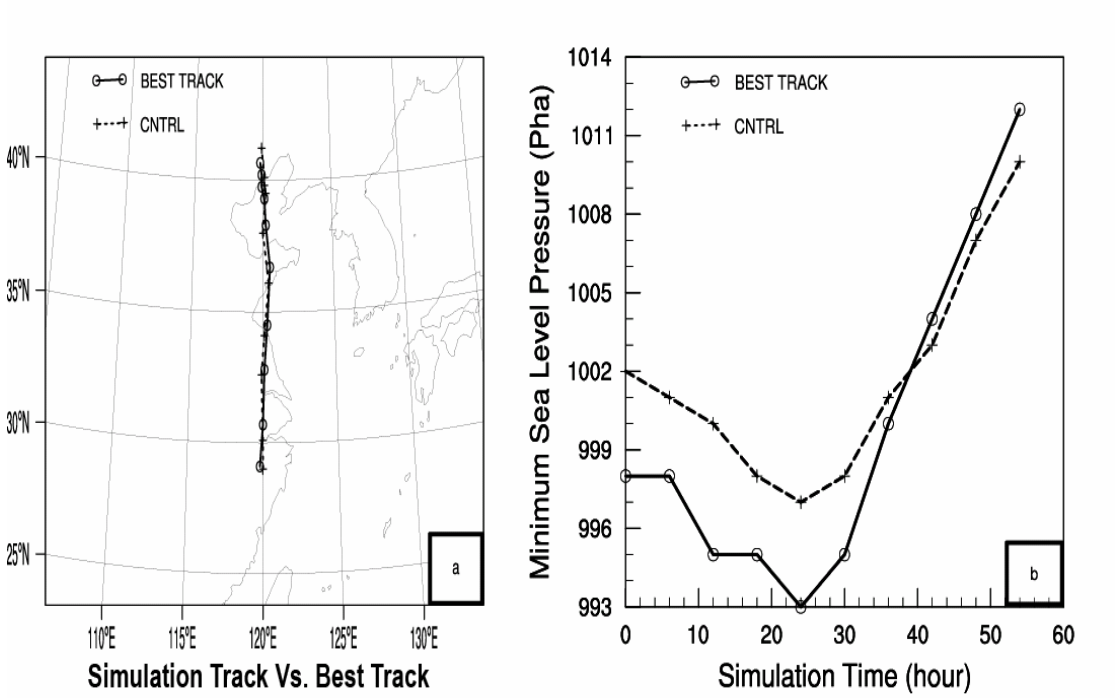

Figure 2. The path (a) and intensity (b) of the best track data and control simulation plotted at 6-h interval. The solid line with circles indicates the best track, while the dashed line with stars is used for the control simulation.

Figure 3a shows that a low vortex lies in the northeast of China (40°N, 123°E) at the initial time. The westward extension of the subtropical high separates the two systems of the low vortex and tropical storm at lower levels, and strengthens the northerly flow in front of Toraji. An upper-level trough over the north of China is associated with a baroclinic zone that interacts with Toraji remnants at the initial time of the simulation. A strong southwesterly jet is evident at 700 hPa, resulting in the storm moving to the north directly (Figure 2a), where wind speeds show local maxima at the entrance and exit regions of the wind jet (Figure 3a). Figure 3b indicates the 72-h total rainfall distribution of the control simulation. The maximum precipitation is located over Shandong with 100-200 mm accumulated precipitation, which is close to the observation (not shown).

The 925-hPa wind vector (taken as the approximate top of the boundary layer) is presented with the low-level 850 hPa PV in Figures 4a, 4c, 4e, and 4g. The 250-hPa wind vector (taken as the upper-tropospheric jet) is also shown with the 850-hPa thickness and column-integrated precipitable water (PW) in Figures 4b, 4d, 4f, and 4h. During the first 12 h of the simulation, the large cold vortex on the 850 hPa level associated with the lower-level southwestern rich relative-humidity bands above East China moves slowly eastward across Northeast China (Figures 4a and 4b). The tropical remnant of Toraji

located over East China (32.6ºN, 119.9ºE) is being intensified gradually as it progresses. A TC is initially observed as positive anomalies in the PV field, whose patterns are modified rapidly by the onset of the frontal precipitation and the distribution of the humidity field with the southwesterly LLJ (Figures 4a, 4c, 4e, and 4g). Toraji undergoes a rapid evolution during the first half of the simulation, as it moves northward and wraps around cyclonically near 120°E. The 850 hPa PV for the tropical remnant strengthens with the moisture transportation for the 24-h and 36-h integration, leading to the re-intensification of Toraji as it enters the Bohai Gulf of China (Figures 4c, 4d, 4e, and 4f). The PW surrounding the remnant vortex reaches the maximum of over 60 mm (Figures 4b, 4d, 4f, and 4h). During this phase of TC life cycle, the tropical system also suffers from the intrusion of the cold front associated with a vortex to its northeast (Figures. 4c and 4e). Figures 4f and 4h for the 48-h simulation display further changes for Toraji. The initial trough in the upstream of Toraji undergoes a rapid cyclonic rollup with the developing lower-level system. And there is an upper-level jet with the speed over 40 m s^{-1}, enhancing the upper-level outflow near the core of the remnant vortex (Figures 4b and 4d). Toraji starts to undergo an ET process after the 24-h simulation (Figure 5). Figure 5 also shows the vertical structure of the tropical remnant's equivalent potential temperature and relative-humidity fields associated with the circulation vectors after the 24-h simulation. As shown in Figure 5, the high moisture air at lower levels and the cold front intrusion at upper levels result in an increase of the convection in the eye wall of the storm, and thus Toraji undergoes a re-intensification while entering the sea again.

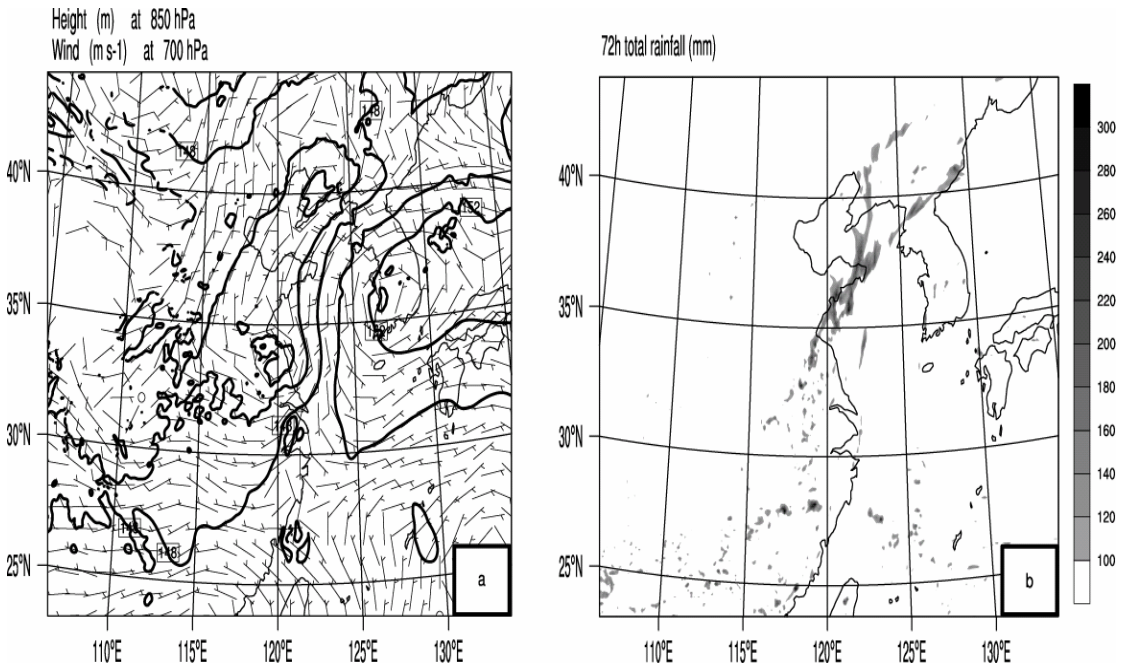

Figure 3. (a) Wind barbs at 700 hPa and thickness at 850 hPa (solid; 2-dam interval) at the initial time, and (b) total rainfall (20-mm interval) after 72 hours of integration.

3 SENSITIVITY TESTS

In this study, four sensitivity simulations are undertaken to evaluate the impact of moisture transportation of environmental southwesterly wind, water vapor carried by the TC itself, trough interaction with a vortex in the northeast of the TC, and the latent heat induced by the oceanic processes that affect Typhoon Toraji's intensity. As shown in Table 1, the first test reduces the relative humidity to 70% around the region of (25–35°N, 115–125°E). The second removes the low vortex near (23°N, 125°E). The third removes the tropical remnant itself. And the fourth reduces the drag coefficient over the sea. Note that the third test is only to remove the anomalies that are clearly identifiable as tropical remnant structure, and the environmental fields remain unchanged. Any significant differences between the results of the control simulation and those of an individual sensitivity test should indicate the role of the process under consideration. The removal algorithm for typhoon vortex used by Ross and Kurihara[28] was adopted in this study, in which a simple smoothing operator of Kurihara et al.[29] was applied successively to the wind, geopotential height, temperature, and specific humidity fields provided by the FNL analysis fields centered at the observed typhoon center for a given time. The low drag coefficient scheme of model TC surface layer used by Zeng et al.[30] was used in this study.

Table 1. Summary of initial condition modifications for each test.

Feature removed	Moisture decrease	Northeast vortex removal	Remnants removal	Low drag coefficient
Experiment	RH70	NOLV	NOTC	LOCD

Figure 6 shows the evolutions of the minimum central sea-surface pressure for the four sensitivity experiments listed in Table 1 except for Exp NOTC, the control simulation, and the best track observed. The simulated TC intensity in these sensitivity tests is weaker than that observed at the initial time, due to the lack of high-resolution data for the initial background fields. Exp RH70 shows that there is a dramatic decreasing trend of the TC intensity, suggesting that the environmental moisture plays an important role in TC intensity change. The TC maintaining period is shortened when the large-scale water-vapor supply is decreased. Exp NOLV indicates that the TC intensity decreases when there is no impact from the low vortex to its northeast, especially during the first 36-h integration. This means that the "good trough" interaction between the tropical remnant and low vortex enhances the TC intensity in this case. Note that there is no TC development when the TC is removed in Exp NOTC. It is interesting that the storm deepens when it moves to the sea at the lower drag coefficient in Exp LOCD.

3.1 *Moisture decrease (RH70)*

The objective of Exp RH70 is to investigate the impact of tropical moisture on the re-intensification of the remnant tropical vortex. Figures 7a, 7c, 7e, and 7g show that TC's PV field, derived from Exp RH70, is constricted to small and narrow regions of the modeled atmosphere. And the wind is also weaker than that in the control simulation. Reduction of the local maximum in the PV field near the core of the decaying vortex results in a reduction of the thickness at 850 hPa (Figure 7b) and a much higher central pressure (1006 hPa) for Typhoon Toraji during the first 24-h simulation at 1200 UTC on 1 August (Figure 6). As shown in Figures 7b, 7d, 7f, and 7h, the PW surrounding the remnant vortex has been decreased by as much as 50 mm (cf. Figures 4b, 4d, 4f, and 4h). A local minimum appears in the PW field over the dry inflow region, so there is a remarkable change in the structure and/or the intensity of the trough. The simulated storm intensity is sensitive to the removal of the tropical moisture structure (Figure 6). In other words, a southwesterly lower-level flow along the coast ahead of the approaching upper-level trough advects the moist air away from the sea toward the redeveloping system after 24-h simulation. As a result, this lower-level moisture ingestion decreases lower-level convective stability to increase convective activity shown in Figure 5. However, if the conveyor belt structure continues to cut off moisture from the tropics as shown in this simulation, the cyclone will have no access to a tropical moisture source for a long period of time and thus is weakened in intensity quickly (Figures 7f and 7g).

3.2 *Northeast vortex removal (NOLV)*

The removal from the initial conditions of the dry PV anomaly associated with the low vortex located to the northeast of the TC shows the influence of the development processes occurring beneath the approaching upper-level trough on Typhoon Toraji circulation and intensity change. As shown in Figures 8a, 8c, 8e, and 8g, the region, selected to exclude only the PV anomalies associated with the low vortex, diminishes in the 850 hPa layer. In Figures 8b, 8d, 8f, and 8h, there is also no upper-level trough jet near the core of the tropical remnant, although the PW is almost the same as that in the control simulation (cf. Figures 4b and 4d). Overall Toraji's intensity in this test is dramatically weaker than in the control simulation, especially during the first 36-h simulation (Figure 6), due to the lack of the merging PV. This means that the low vortex in this case is also very important for strengthening the remnant vortex. Note that Toraji's intensity in this test starts to become stronger than that in the control run after 36-h simulation (Figure 6), because the effect of the removed low vortex on TC intensity decreases in time (Figures 8e and 8g).

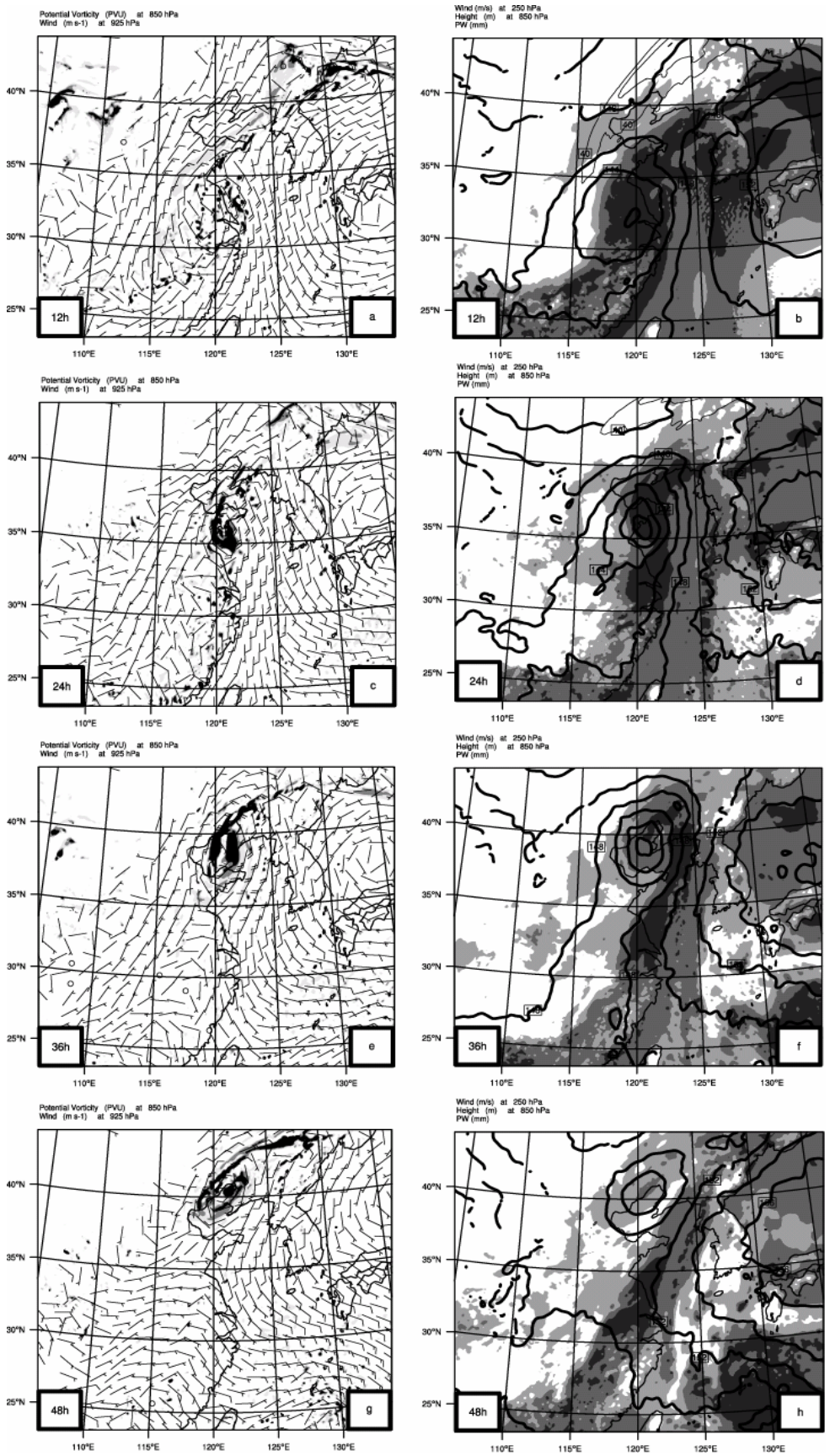

Figure 4. (Left) The 925-hPa wind vector and 850-hPa PV (shadings for absolute values greater than 1, 1.5, and 2 PVU) after (a) 12, (c) 24, (e) 36, and (g) 48 h. (Right) The 250-hPa wind speed (light solid for greater than 40, and 50 m s^{-1}), 850-hPa thickness (heavy solid; 2-dam interval) and column-integrated precipitable water (shading at 10-mm interval above 40 mm) after (b) 12, (d) 24, (f) 36, and (h) 48 h.

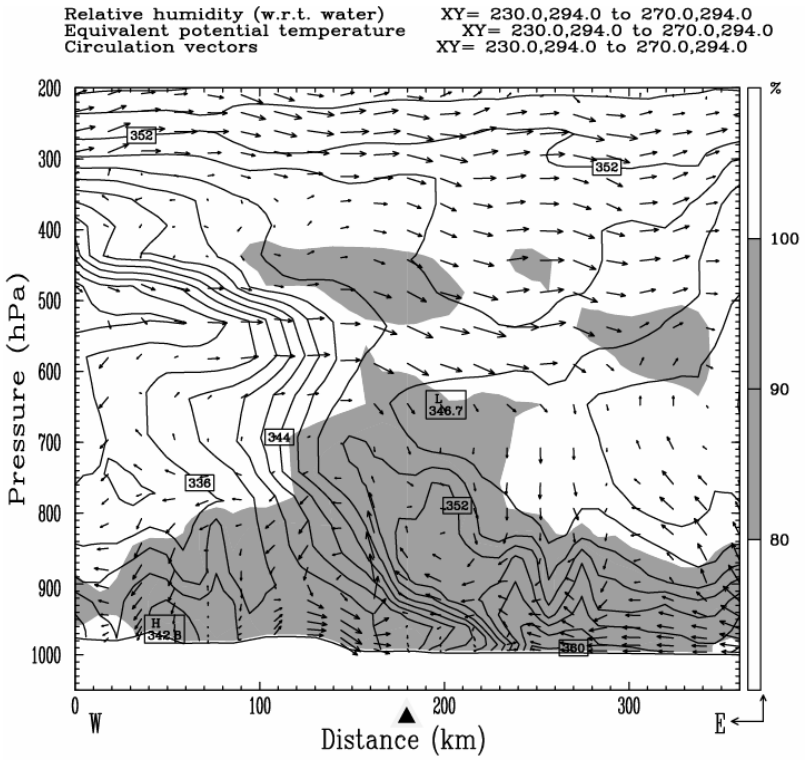

Figure 5. Vertical profile of the equivalent potential temperature (solid; 2-K interval), relative humidity (shading at 10% interval above 80%), and circulation vectors crossing the center of tropical remnant from west to east after 24-h integration. Note that the solid triangle indicates the location of tropical remnant.

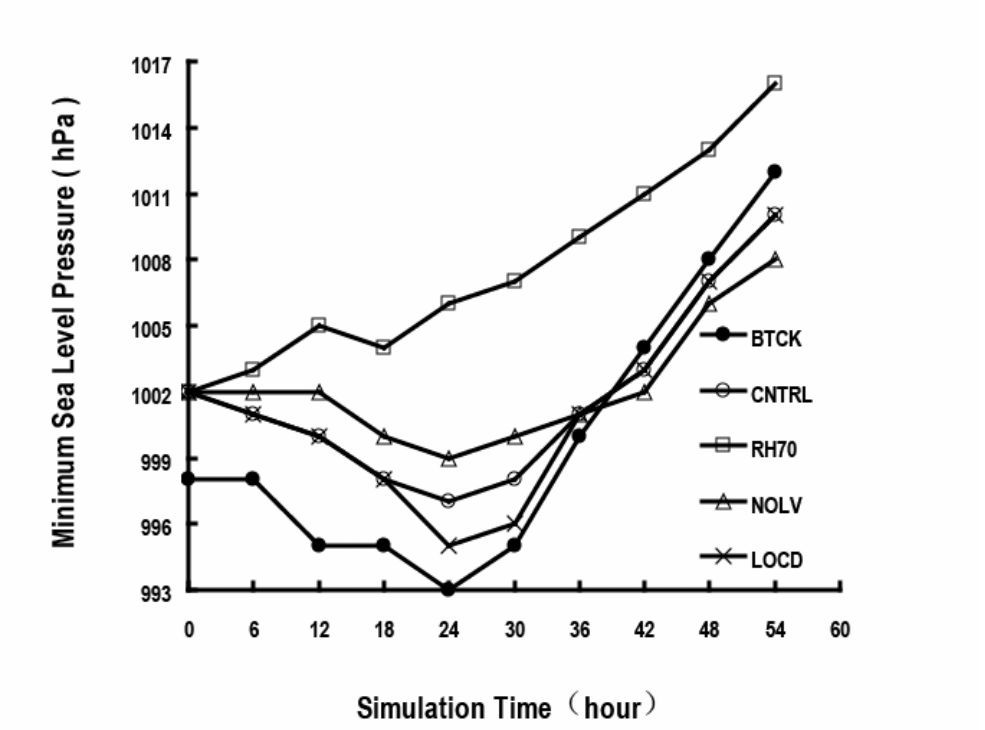

Figure 6. The evolution of the minimum central sea-surface pressure (hPa) in the four experiments listed in Table 1, except for Exp NOTC, the control simulation, and the best track (solid circle) plotted at 6-h interval. Shown are the control simulation (CNTRL) plotted with open circles, Exp RH70 with squares, Exp NOLV with triangles, and Exp LOCD with crosses. Note that there is no TC development when the TC is removed in Exp NOTC.

3.3 *Remnant's removal (NOTC)*

The objective of Exp NOTC is to quantify the influence of the remnant tropical circulation on the re-intensification process. Removal of the initial lower-level PV anomaly associated with Toraji leads to an increase of geopotential height at the surface and thickness reductions (Figure 9). During the first 12-h

simulation, a small incipient surface cyclonic inversed trough forms near 26°N, 110°E (Figure 9b), which travels slowly eastward under the influence of a pre-existing extratropical low vortex over Northeast China. Shortly afterwards, the incipient vortex circulation forms in the southwest of the original low center, but has no intensification (Figures 9d, 9f, and 9h). During the 48-h simulation (Figure 9), there is little evidence of the filamentation and wrapping processes at lower levels in the control simulation. Elevated PV does not penetrate northward to the east of the developing system since the low-level circulation, responsible for the advection of tropical air ahead of the system, has been removed. The tightly rolled lower-level PV structure, observed in the control simulation around Toraji, is not developed in this test simulation. Instead, a moderately intense warm front extends northeastward from the cyclone's circulation, and a cold front moves eastward to 130°E (Figures 9b, 9d, and 9f). At all levels, the evolutionary differences between Exp NOTC and the control run are striking. Instead of the tropical-mode re-intensification diagnosed in the control run, the simulated system in Exp NOTC develops a weak baroclinic cyclone with little support from the predominantly linear processes aloft.

3.4 *Low drag coefficient (LOCD)*

Typhoon Toraji's structure and intensity changes are also affected by the conditions of the TC boundary layer (Zeng et al.[30]). The objective of Exp LOCD is to evaluate the effect of the boundary layer process on TC intensity change. Figure 6 shows that the storm with a small drag coefficient has deepened while moving to the sea, which locally enhances oceanic latent-heat flux, leading to convective instability over the dry region. The flux exceeds 240 W m^{-2} after 24 h (not shown), while the flux in the control run remains below160 W m^{-2} (not shown). Figures 10a and 10b show that the sensible- and latent-heat fluxes in Exp LOCD are larger than those in the control simulation after 24-h integration, especially over the sea. Figures 10c and 10d indicate similar patterns after 36-h simulation to those after 24-h simulation, with the impact region enlarged after 36-h simulation. Once the moistened boundary layer becomes potentially unstable beneath the dry air aloft, an outbreak of convection occurs. No such widespread enthalpy heat-flux enhancement is observed in Exps RH70, NOLV, and NOTC where the primary moistening process is advection. Therefore, the increasing surface flux enhances convective destabilization in Exp LOCD, suggesting that the drag coefficient is very important for TC intensity change (Zeng et al.[30]).

4 EFFECT ON RAINFALL

Water vapor is a key element for precipitation. Different distributions of water vapor have strong influence on TC's rainfall pattern. Figure 11 shows the 72-h accumulated rainfall in all the experiments listed in Table 1. Comparing with the control simulation, the rain belt is obviously narrower, and the precipitation intensity is also smaller in Exp RH70 (Figure 11a). In Exp NOLV without the impact of the northeast low vortex, there is a wider rain belt northward with somewhat larger rainfall than that in the control run (Figure 11b). For Exp NOTC without the tropical remnant circulation, the rain belt is constricted and the rainfall amount is also smaller than that in the control simulation (Figure 11c), which indicates that the rich water vapor carried by the TC is also a major supplier for the TC precipitation. The rain pattern in Exp LOCD is almost the same as that in the control simulation, except for the rain intensity that is increased by 8% for the maximum precipitation (Figure 11d), which results in an increase of the outer rain band and diabatic heat release due to the latent heat. Correspondingly, the vertical structure of the equivalent potential temperature, relative humidity, and circulation vectors, crossing the center of the tropical remnant from west to east after 24-h simulation in all the experiments listed in Table 1, show different convection instability as does the control simulation (Figure 12). The biggest convection instability is seen in Exp LOCD after 24-h simulation (Figure 12d). Therefore, the TC remnant in Exp LOCD brings the largest amount of rainfall over Shandong province.

5 EVOLUTION OF MOISTURE FLUX DIVERGENCE

The column-integrated moisture flux divergence is a good measure of whether or not the northward-transported moisture contributes to the precipitation (Banacos and Schultz[31]) in all the experiments listed in Table 1 as well as in the control simulation. At a given time, the column-integrated moisture flux divergence can be expressed as

$$M = \int_0^{z_t} \nabla \cdot (\rho q_v V) \mathrm{d}z \qquad (1)$$

where V is the horizontal wind vector, z is the height, and z_t is the height of the model top; q_v is the water vapor mixing ratio, and ρ is the air density. Figure 13 shows the column-integrated moisture flux divergence during 72-h simulation from all the experiments listed in Table 1 and the control simulation over part of Shandong province (35–38°N, 118–124°E).

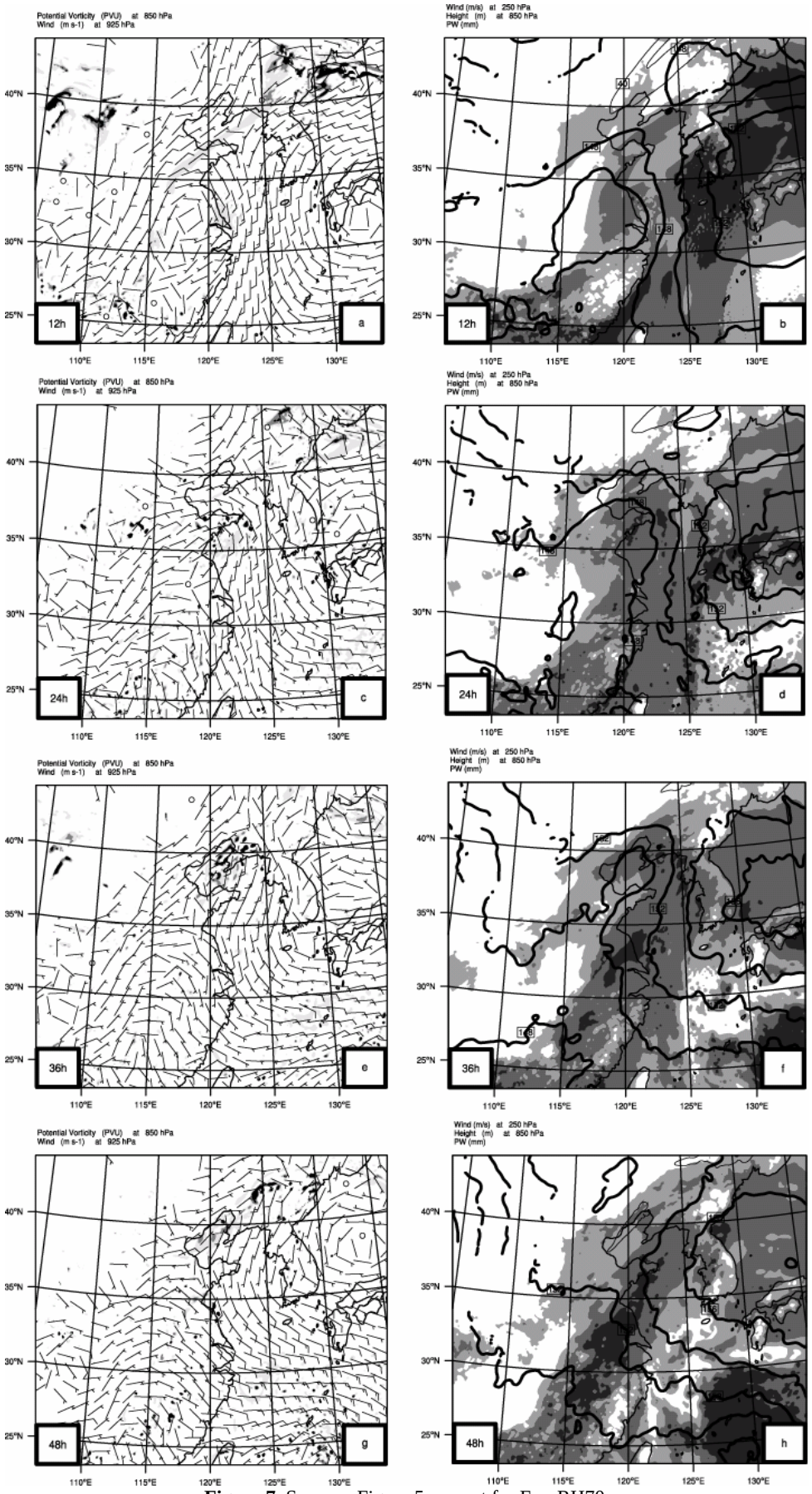

Figure 7. Same as Figure 5, except for Exp RH70.

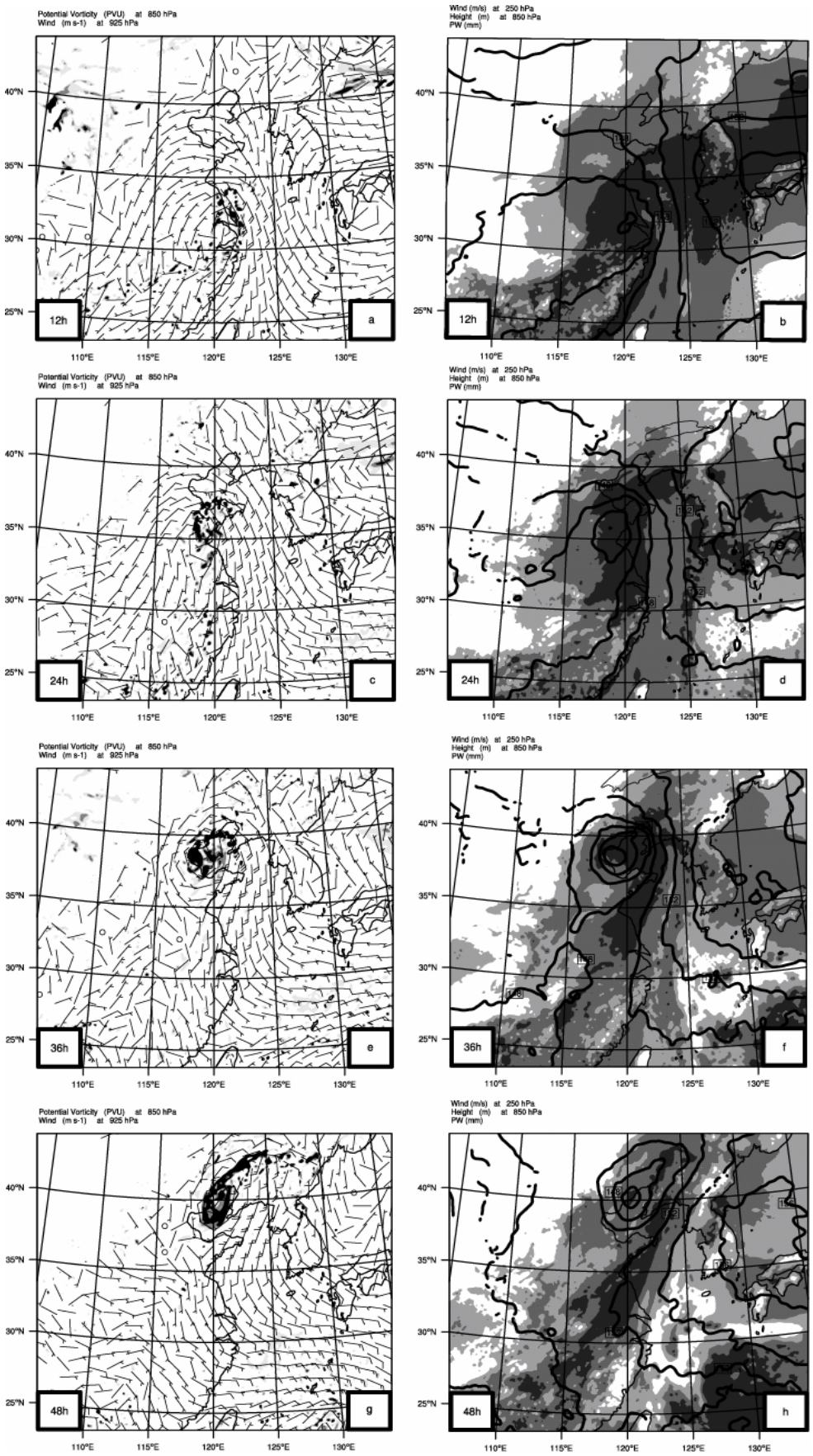

Figure 8. Same as Figure 5, except for Exp NOLV.

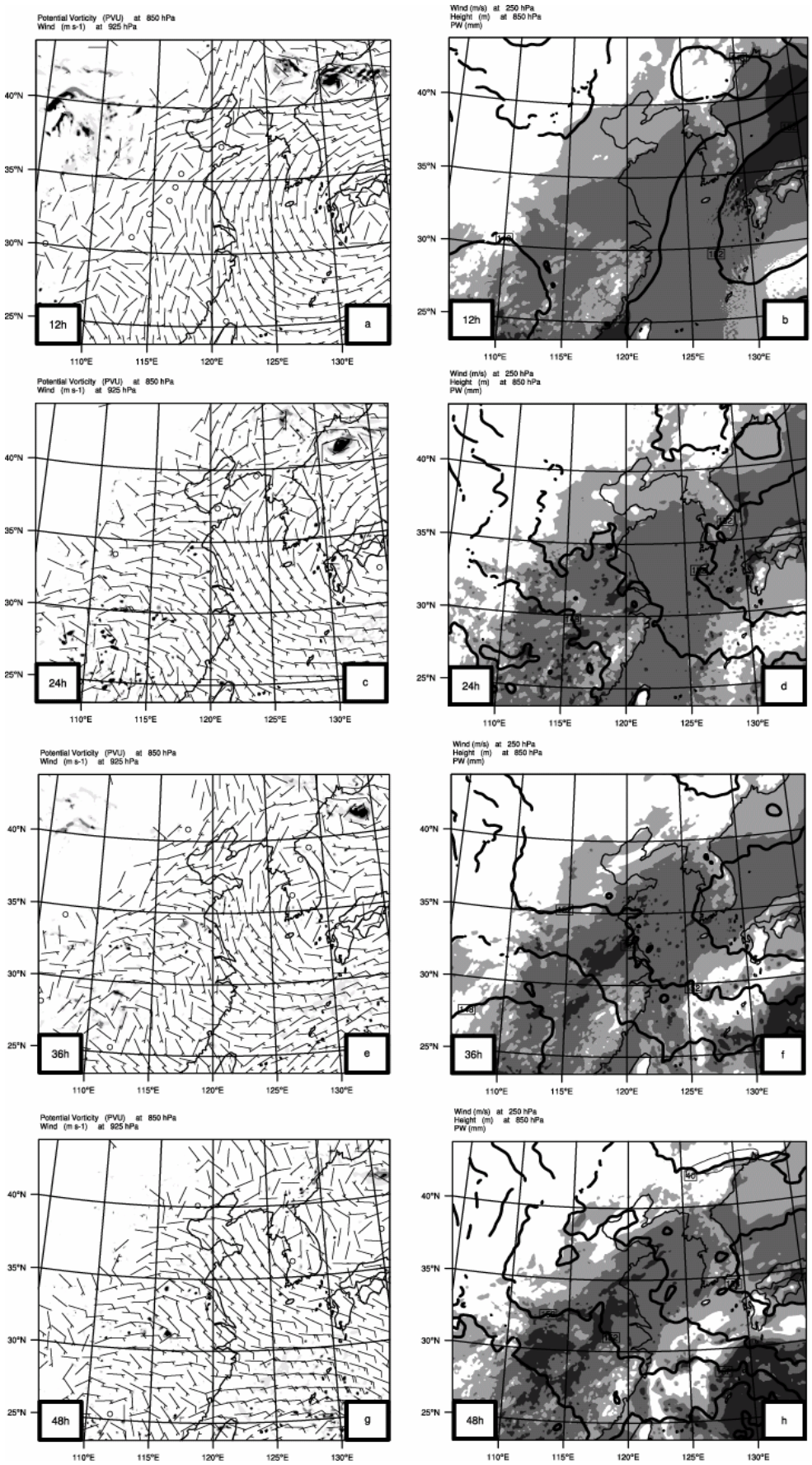

Figure 9. Same as Figure 5, except for Exp NOTC.

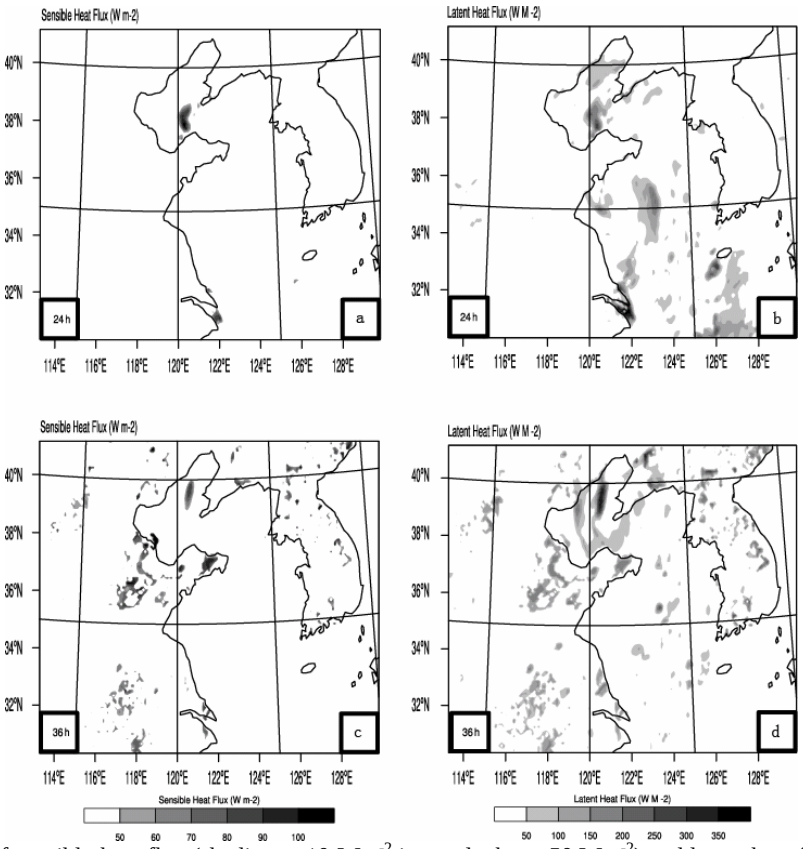

Figure 10. Differences of sensible-heat flux (shading at 10-Wm^{-2} interval, above 50 Wm^{-2}) and latent-heat flux (shading at 50-Wm^{-2} interval, above 50 Wm^{-2}) between the low drag coefficient simulation and the control simulation after (a, b) 24-h and (c, d) 36-h integrations.

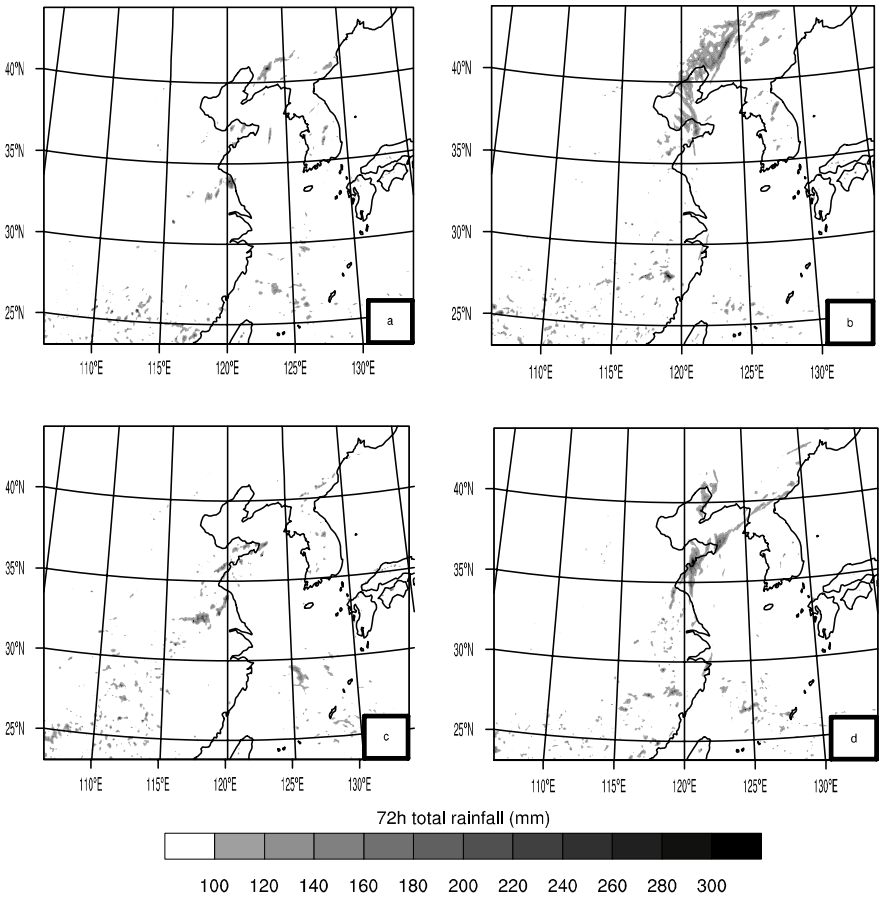

Figure 11. The 72-h total accumulated rainfall (shading at 20-mm interval, above 100 mm) in all the experiments listed in Table 1. Shown are (a) Exp RH70, (b) Exp NOLV, (c) Exp NOTC, and (d) Exp LOCD.

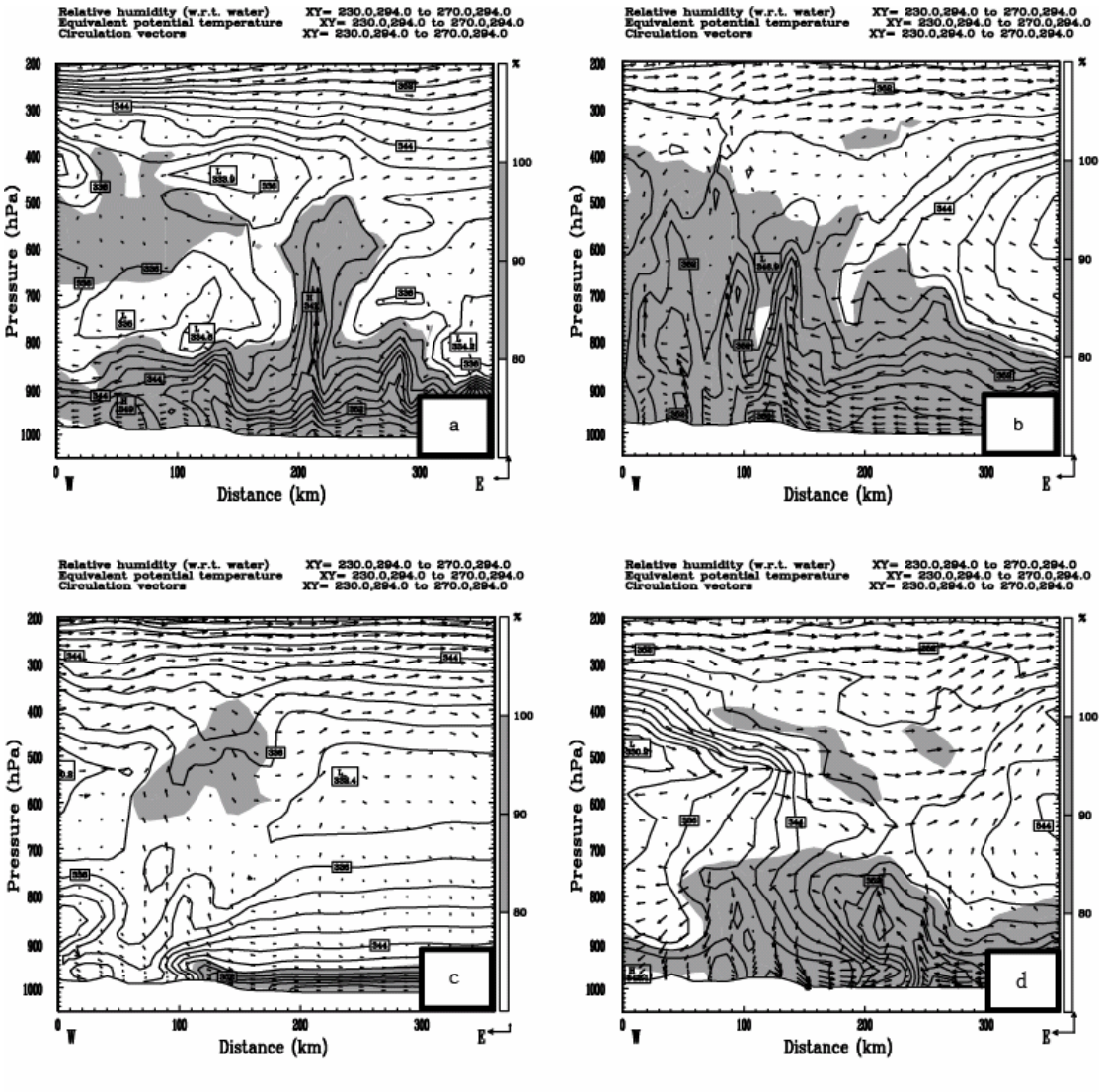

Figure 12. Same as Figure 6, except for all the experiments listed in Table 1. Shown are (a) Exp RH70, (b) Exp NOLV, (c) Exp NOTC, and (d) Exp LOCD.

Figure 13 shows that the TC remnant alternatively maintains and intensifies because of an increase in the moisture flux convergence induced by the lower-level southwesterly jet, although the moisture transfer is decreased over the land during the first 18-h simulation. From 24-h to 36-h simulation, the moisture flux convergence grows again due to the combination effect of southwesterly jet and the warm and wet air over the sea, which results in the remnant vortex's re-intensification. The minimum central sea surface pressure in Exp NOLV is stronger than that in the control simulation, because the moisture flux convergence in Exp NOLV increases significantly after 36-h simulation. However, there is little change in moisture transportation in Exp NOTC (without the TC circulation). The tendency of the moisture flux convergence in Exp RH70, with a large amplitude change, is similar to the temporal evolution in Exp NOTC. Note that the temporal evolution of the moisture flux convergence in Exp LOCD is almost the same as that in the control simulation, except with a larger amount of the moisture flux convergence from 24-h to 36-h simulation than that from the control run, leading to an enhancement of the latent-heat flux (see Figure 10b). Comparing Figure 13 with Figure 6, one can find that the tropical remnant re-intensification is well correlated with the column-integrated moisture flux convergence with lags from about 12 to 18 h, which implies that it should take some time for TC intensity change to response to the large-scale environmental change.

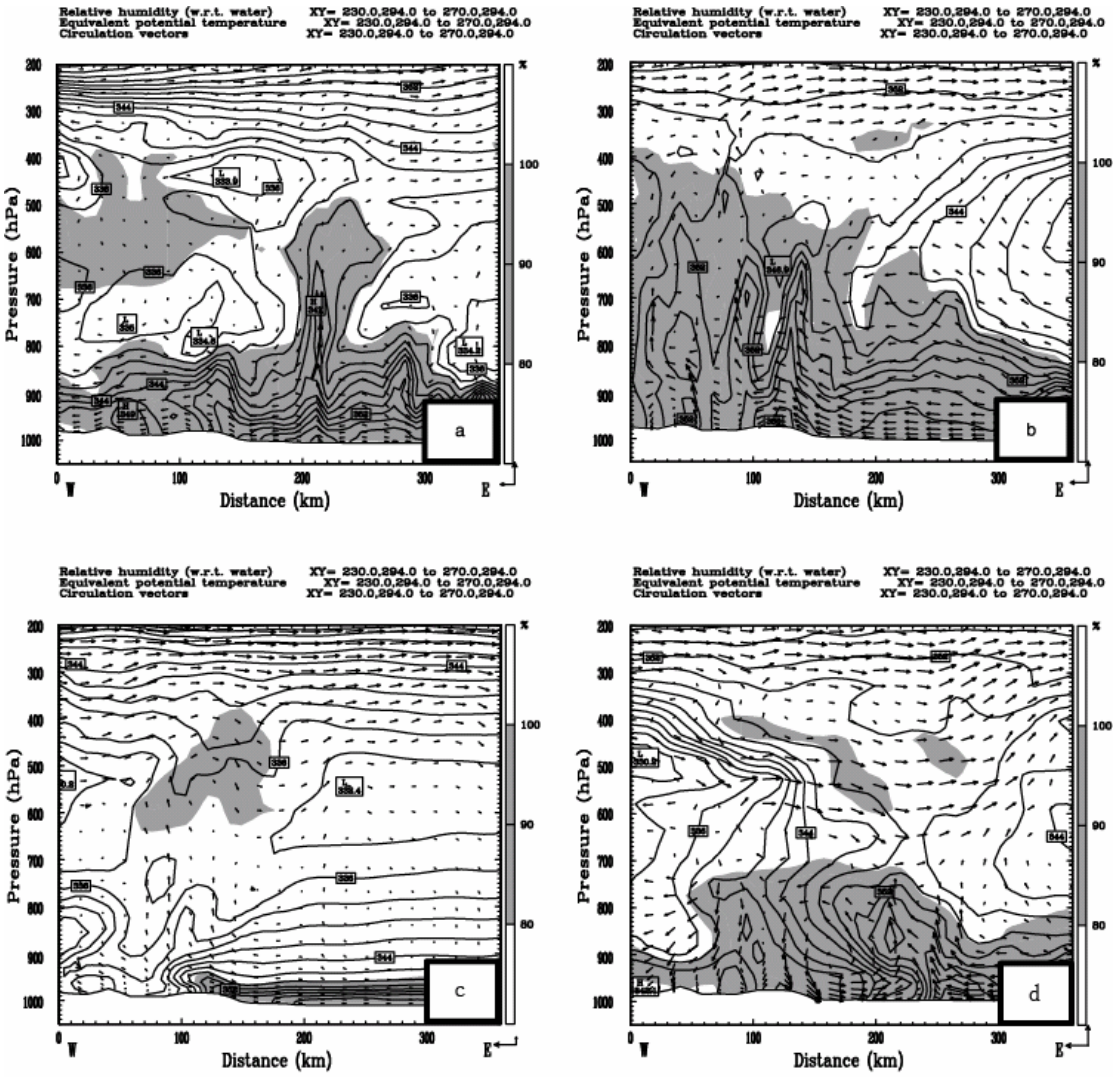

Figure 13. The column-integrated moisture flux divergence (1000 g m^{-2} s^{-1}) during 72-h simulation from all the experiments listed in Table 1 and the control simulation. Shown are the control run (CNTRL) plotted with circles, Exp RH70 with squares, Exp NOLV with triangles, Exp NOTC with crosses, and Exp LOCD with stars.

6 SUMMARY AND DISCUSSION

The Advanced Research WRF model is used to investigate the effects of environmental factors on Typhoon Toraji (2001) re-intensification after returning to the sea, including moisture transportation, the upper-level trough interaction with PV anomalies, tropical remnant circulation, and TC boundary layer process. In the case when Typhoon Toraji was located in the Bohai Gulf of China, heavy rainfall occurred over Shandong province in China along the adjacent sea. In the control experiment with a traditional drag coefficient algorithm, the model reasonably described the major features of Typhoon Toraji and the precipitation over Shandong. Four sensitivity experiments were performed in order to explicitly demonstrate the contributions of the moisture transfer from southwesterly lower-level jet, the northeast low vortex with PV anomalies, tropical remnant circulation, and low drag coefficient scheme for Typhoon Toraji's intensity change while moving from land to sea. The PV merging, moisture flux convergence, and the precipitation zone and intensity were largely suppressed, thus weakening Toraji's intensity, due to the removal of relative humidity by 70% in the model atmosphere and removal of tropical remnant circulation at the initial time. The tropical remnant intensity is dramatically weaker than that of the control simulation, especially during the first 36-h simulation. This arises from the fact that the model has removed the impact of the northeast low vortex, leading to the reduction of PV merging.

In this case study, the major process involved in the intensity change of Typhoon Toraji is through the enhanced northward moisture transport into the preconditioned precipitation region by the large-scale environmental conditions and the outer circulation. The results show that moisture transfer by a

southwesterly jet, a northeast low vortex, and the presence of Typhoon Toraji were critical to the simulated heavy rainfall over Shandong and remnant re-intensification after it returned to the sea. In the experiment with the low drag coefficient scheme, the overall precipitation pattern and intensity change were very similar to those from the control simulation except for an 8% overestimate of the precipitation, especially in the period over the sea, indicating that the local boundary layer forcing played a secondary role in the case studied.

REFERENCES:

[1] CHEN Lian-shou, DING Yi-hui. Introduction to the Western Pacific typhoons (in Chinese) [M]. Beijing: Science Press, 1979: 491pp.

[2] POWELL M D. The transition of the hurricane Frederic boundary-layer wind field from the open Gulf of Mexico to landfall [J]. Mon. Wea. Rev., 1982, 110(12): 1912-1932.

[3] POWELL M D. Changes in the low-level kinematic and thermodynamic structure of hurricane Alicia (1983) at landfall [J]. Mon. Wea. Rev., 1987, 115(1): 75-79.

[4] POWELL M D, HOUSTON S H. Surface wind fields of 1995 hurricanes Erin, Opal, Luis, Marilyn, and Roxanne at landfall [J]. Mon. Wea. Rev., 1998, 126(5): 1259-1273.

[5] TULEYA R E. Tropical storm development and decay: Sensitivity to surface boundary conditions [J]. Mon. Wea. Rev., 1994, 122(2): 291-304.

[6] TULEYA R E, BENDER M A, KURIHARA Y. A simulation study of the landfall of tropical cyclones using a movable nested-mesh model [J]. Mon.Wea. Rev., 1984, 112(1): 124-136.

[7] SHEN W, GINIS I, TULEYA R E. A numerical investigation of land surface water on landfalling hurricanes [J]. J. Atmos. Sci., 2002, 59(4): 789-802.

[8] CHEN Lian-shou. Decay after landfall [M]. WMO/TD, 1998: 875, 1.1.6-1.1.7.

[9] DING Yi-hui, LIU Yi-zong. Study on the moisture budget in typhoon (7507) [J]. Acta Oceanol. Sinica, 1986, 8(3): 291-301.

[10] TAN Ran-zi, LIANG Bo-qi, Comparative study on the decaying and the extratropical transition of making landfall typhoon [J]. J. Sun Yat-sen Univ. (Nat. Sci.), 1989, 28(4): 15-21.

[11] EMANUEL K A. The maximum intensity of hurricane [J]. J. Atmos. Sci., 1988, 45(7): 1143-1155.

[12] HOLLAND G J. The maximum potential intensity of tropical cyclone [J]. J. Atmos. Sci., 1997, 54(21): 2519-2541.

[13] WANG Y Q, WANG Y, FUDEYASU H. The role of Typhoon Songda (2004) in producing distantly located heavy rainfall in Japan [J]. Mon. Wea. Rev., 2009, 137(11): 3699-3716.

[14] HOLLAND G J, MERRILL R T. On the dynamics of tropical cyclone structural changes [J]. Quart. J. Roy. Meteor. Soc. 1984, 110(465): 723-745.

[15] MOLINARI J, VOLLARO D. External influences on hurricane intensity. Part I: Outflow layer eddy angular momentum fluxes [J]. J. Atmos. Sci., 1989, 46(8): 1093-1105.

[16] Molinari J, VOLLARO D. External influences on hurricane intensity. Part II: Vertical structure and response of hurricane vortex [J]. J. Atmos. Sci., 1990, 47(15): 1902-1918.

[17] PERSING J, MONTGOMERY M T, TULEYA R E. Environmental interactions in the GFDL hurricane model for Hurricane Opal [J]. Mon. Wea. Rev., 2002, 130(2): 298-317.

[18] HANLEY D E, MOLINARI J, KEYSER D. A composite study of the interaction between tropical cyclones and upper tropospheric troughs [J]. Mon. Wea. Rev., 2001, 129(10): 2570-2584.

[19] GUO Li-xian, CHEN Lian-shou, LI Ying, et al. Statistical characteristics of intensity change of tropical cyclones landing in China before moving out to sea [J]. J. Trop. Meteor., 2010, 26(1): 65-70.

[20] SKAMAROCK W C, KLEMP J B. A time split non hydrostatic atmospheric model for weather research and forecasting applications [J]. J. Comp. Physics., 2008, 227(7): 3465-3485.

[21] FERRIER B S. A double-moment multiple-phase four-class bulk ice scheme. Part I: Description [J]. J. Atmos. Sci., 1994, 51(2): 249-280.

[22] MLAWER E J, TAUBMAN S J, BROWN P D, et al. Radiative transfer for inhomogeneous atmosphere: RRTM, a validated correlated-k model for the long-wave [J]. J. Geophys. Res., 1997, 102 (D14), 16663-16682.

[23] CHOU M D, SUAREZ M J. An efficient thermal infrared radiation parameterization for use in general circulation models (Vol. 3) [M]. NASA Tech. Memo. 104606, 1994: 85pp.

[24] SMIRNOVA T G, BROWN J M, BENJAMIN S G. Performance of different soil model configurations in simulating ground surface temperature and surface fluxes [J]. Mon. Wea. Rev., 1997, 125(8): 1870-1884.

[25] SMIRNOVA T G, BROWN J M, BENJAMIN S G, et al. Parameterization of cold-season processes in the MAPS land-surface scheme [J]. J. Geophys. Res., 2000, 105 (D3), 4077-4086.

[26] HONG S Y, NOH Y, DUDHIA J. A new vertical diffusion package with an explicit treatment of entrainment processes [J]. Mon. Wea. Rev., 2006, 134(9): 2318-2341.

[27] KAIN J S, FRITSCH J M. A one-dimensional entraining/detraining plume model and its application in convective parameterization [J]. J. Atmos. Sci., 1990, 47(23): 2784-2802.

[28] ROSS R J, KURIHARA Y. A numerical study on influences of Hurricane Gloria (1985) on the environment [J]. Mon. Wea. Rev., 1995, 123(2): 332-346.

[29] KURIHARA Y, BENDER M A, TULEYA R E, et al. Prediction experiments of Hurricane Gloria (1985) using a multiply nested movable mesh model [J]. Mon. Wea. Rev., 1990, 118(10): 2185-2198.

[30] ZENG Zi-hua, WANG Yan, DUAN Yi, et al. On sea surface roughness parameterization and its effect on tropical cyclone structure and intensity [J]. Adv. Atmos. Sci., 2010, 27(2): 337-355.

[31] BANACOS P C, SCHULTZ D M. The use of moisture flux convergence in forecasting convective initiation: Historical and operational perspectives [J]. Wea. Forecasting, 2005, 20(3), 351-366.

Citation: ZENG Zhi-hua and CHEN Lian-shou. Numerical simulation on re-intensification of tropical remnant re-entering the sea: A case study. *J. Trop. Meteor.*, 2012, 18(2): 146-161.